Acta Pharmacologica Sinica (2009) 30: 1033–1038

www.nature.com/aps

Original Article

Marine-derived oligosaccharide sulfate (JG3) suppresses heparanase-driven cell adhesion events in heparanase over-expressing CHO-K1 cells

Qiu-ning LI, Hai-ying LIU, Xian-liang XIN, Qiu-ming PAN, Lu WANG, Jing ZHANG, Qin CHEN, Mei-yu GENG*, Jian DING*

Division of Anti-Tumor Pharmacology, State Key Laboratory of Drug Research, Shanghai Institute of Materia Medica, Shanghai Institutes for Biological Sciences, Chinese Academy of Sciences, Shanghai 201203, China

Aim: To elucidate the detailed mechanisms underlying the appreciable effects of JG3, a novel marine-derived oligosaccharide, on cell migration using a Chinese hamster ovary (CHO) cell line stably over-expressing heparanase.
Methods: A retrovirus infection system was used to establish a CHO-K1 cell line stably transfected with heparanase. Immunocytochemistry was used to assess cell morphology. Flow cytometry was selected to analyze the activation of β1-integrin, and Western blotting was used to analyze the downstream effects on the cell adhesion pathway. An affinity precipitation assay was used to determine activation of the small GTPases, Rac1, and RhoA.
Results: JG3 abolished heparanase-driven formation of focal adhesions and cell spreading. Although JG3 failed to block the heparanase-triggered activation of β1-integrin or the phosphorylation of Src, the oligosaccharide caused a significant dephosphorylation of FAK and subsequent inactivation of Erk. Furthermore, JG3 was found to arrest the activation of Rac1.
Conclusion: All these findings help form an alternative view to understand the mechanisms underlying the inhibitory effects of JG3 on cell motility.

Keywords: JG3; heparanase; cell adhesion; cell motility

Acta Pharmacologica Sinica (2009) 30: 1033–1038; doi: 10.1038/aps.2009.97; published online 22 June 2009

Introduction

Heparanase is an endo-β-*D*-glucuronidase capable of partially depolymerizing heparan sulfate (HS) side chains. Pathologically, heparanase has been commonly accepted to be associated with the metastatic potential of tumor-derived cells, as a consequence of HS cleavage and the resulting disruption of the extracellular matrix (ECM) barrier[1–4]. Further investigation has revealed that heparanase is correlated with vascular density and shorter postoperative survival in cancer patients. All these data provide strong clinical support for the prometastatic and proangiogenic functions of the enzyme and position heparanase as an attractive target for the development of anticancer drugs[5–8]. In addition, recent evidence has emerged that underscores the non-catalytic feature of the enzyme; in particular, heparanase was noted to enhance cell adhesion via activation of β1-integrin, FAK phosphorylation and Rac1 activation[9–11].

Previous results from our group revealed that JG3, a novel marine-derived oligosaccharide, significantly inhibited heparanase activity in a concentration-dependent manner by specifically binding to the KKDC and QPLK motifs of heparanase. Importantly, we found that JG3 targeted lung metastasis in a murine B16F10 experimental metastasis model, as well as angiogenesis and lung metastasis of MDA-MB-435 orthotopic xenografts in athymic mice[12]. Of these events, JG3 was particularly noted to arrest cell migration, which prompted us to investigate the possible mechanisms involved.

In the present study, we showed that JG3 abolishes heparanase-driven formation of focal adhesions and cell spreading. Further studies indicated that JG3 caused a significant inactivation of FAK, Erk, and the small GTPase Rac1. However, JG3 failed to block β1-integrin activation and Src phosphorylation.

Materials and methods

Materials

JG3 was synthesized and prepared by our lab[12]. Briefly, hydrogen peroxide-degraded oligomannurarate from sodium alginate was reacted with sulfating reagents containing forma-

* To whom correspondence should be addressed.
E-mail mygeng@mail.shcnc.ac.cn (Mei-yu GENG),
suozhang@mail.shcnc.ac.cn (Jian DING)
Received 2009-05-07 Accepted 2009-05-20

mide and $ClSO_3H$. The products were desalted and analyzed via high-performance gel permeation chromatography with a G3000PWxl column (300×7.8 mm; Tosoh, Tokyo, Japan). The structure of MS80 is shown in Figure 1. It is composed of *D*-mannurarate by β(1–4) glycosidic linkage, with sulfate modification of the hydroxyl group at the C2/C3 position. The antibodies to RhoA, Rac1, paxillin, and β1-integrin were obtained from Santa Cruz Biotechnology (CA, USA), and anti-phospho-FAK, anti-non-phospho-FAK, anti-phospho-Erk1/2, anti-non-phospho-Erk1/2, anti-β-actin were purchased from Cell Signaling Technology. Other antibodies included anti-active β1-integrin 12G10 (Serotec, Oxford, UK), FITC-labeled goat anti-rabbit IgG, and FITC-labeled goat anti-mouse IgG (Chemicon International Inc, Temecula, CA, USA). Fibronectin was purchased from Calbiochem (San Diego, CA, USA); laminin, collagen and vitronectin were from Sigma (St Louis, MO, USA).

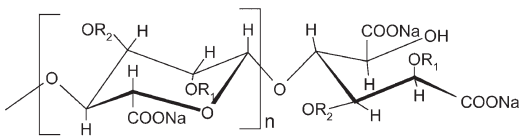

R_1=SO_3Na, R_2=SO_3Na or H, n=3–9

Figure 1. Chemical structure of JG3. The oligosaccharide is composed of *D*-mannurarate by a β(1-4)glycosidic linkage, with sulfate modification of the hydroxyl group at the C2/C3 position.

Cells and cell culture

The retroviral packaging 293T cell line and Chinese hamster ovary cell line (CHO-K1) were purchased from American Type Culture Collection (Rockville, MD, USA). 293T cells were grown in Dulbecco's modified Eagle's medium and CHO-K1 cells were maintained in F12 medium (Gibco, Grand Island, NY, USA). Both media were supplemented with 10% heat-inactivated fetal bovine serum and antibiotics (100 U/mL penicillin, 100 μg/mL streptomycin), and cells were maintained in a 5% CO_2 humidified atmosphere at 37 °C.

Transfection

The generation of high-titer, helper-free retroviruses by transient transfection was achieved by using the highly transfectable 293T cell line. Using Lipofectamine 2000 (Invitrogen) according to the manufacturer's instructions, these cells were transfected with either a pBABE-puro vector that expresses retroviral packaging functions fused with the full-length heparanase cDNA gene (cloned in our lab) in the multiple cloning site or a control pBABE-puro vector, kindly provided by the Bob Weinberg lab. Six hours after transfection, the medium was replaced with fresh medium, and cells were incubated in 5% CO_2 at 32 °C to increase the retroviral titer. Supernatants were collected 48 h later and then filtered with a 0.45-μm pore size filter, stored at -80 °C or used immediately. Equal volumes of virus suspension and polybrene were centrifuged at 1000×*g* for 30 min, then added to the CHO-K1 cells and incubated at 37 °C for 5 h. Then, the suspension was replaced with CHO-K1 medium and the cells were incubated in a 5% CO_2 humidified atmosphere at 37 °C for 48 h. Transfected cells were selected with puromycin (10 μg/mL) for 2 weeks, and stable populations of heparanase-expressing cells were obtained and maintained in growth medium containing 5 μg/mL puromycin to avoid the overgrowth of nontransfected cells. Expression of heparanase was evaluated by reverse transcriptase polymerase chain reaction (RT-PCR) and Western blotting.

Cell adhesion assay

96-well microtiter plates were coated with 0.1 mL human plasma fibronectin (1 μg/mL) in serum-free F12 medium and incubated at 4 °C overnight. On the next day, the unbound human plasma fibronectin was removed and the wells were blocked with 2% BSA at 37 °C for 1 h. Cells suspended in serum-free F12 medium were added to each fibronectin-coated well (3×10^4 cells per well) and incubated at 37 °C for 1 h. The wells were gently washed three times with 200 μL of pre-warmed PBS to remove unbound cells, and then adherent cells were fixed with methanol for 10 min. Cells were then stained with 0.1% crystal violet for 20 min and washed with PBS. The crystal violet dye retained on the wells was removed with 10% acetic acid, and the absorbance of each well at 595 nm was measured using a multiwell spectrophotometer (VERSAmax; Molecular Devices, Sunnyvale, CA, USA).

Immunocytochemistry

Cells were trypsinized and washed with PBS, then resuspended in FBS-free F12 medium with or without 100 μg/mL JG3. The cell suspension was seeded on fibronectin-coated glass coverslips in a 24-well plate for 1 h at 37 °C (1×10^6 cells per well), fixed with 4% paraformaldehyde in PBS for 15 min, and permeabilized with 0.5% Triton X-100 in PBS for 1 min. Cells were then washed with PBS and subsequently incubated in PBS containing 10% normal goat serum for 1 h at room temperature, followed by a 2 h incubation with the indicated primary antibody. Cells were then extensively washed with PBS and incubated with the relevant (Cy2/Cy3-conjugated) secondary antibody (Jackson ImmunoResearch, West Grove, PA, USA) for 1 h. For actin staining, cells were fixed and permeabilized as above, and after being washed three times with PBS, they were incubated with FITC-conjugated phalloidin (Sigma) for 30 min. Slides were mounted in Vectashield antifade medium (Vector Laboratories, Burlingame, CA, USA) and viewed using a confocal microscope (Leica, Mannheim, Germany).

Western blotting

Cells were seeded on fibronectin coated 6-well plates with JG3 for 1 h as described above. After the incubation, cells were washed (×3) with serum-free medium, the remaining attached cells were lysed with RIPA buffer [1% NP-40, 0.5% sodium deoxycholate, 0.1% SDS, 150 mmol/L NaCl, 50 mmol/L Tris

(pH 8.0), 10 μg/mL aprotinin, 10 μg/mL leupeptin, 1 mmol/L phenylmethylsulfonyl fluoride, 1 mmol/L sodium orthovanadate], and the protein concentration was quantified by the BCA™ protein assay reagent kit (Pierce Biotech, Rockford, IL, USA). Cell lysates in 2×SDS loading buffer were subjected to SDS-PAGE and transferred to PVDF membranes. After blocking with 5% BSA in TBST, the membranes were incubated with the appropriate primary antibody (1:1000) in TBST buffer for 2 h at room temperature. After being washed three times in TBST, the membranes were probed with HRP-conjugated anti-rabbit or anti-mouse IgG (1:2000) for 1 h followed by another three TBST washes. Protein bands were visualized by enhanced chemiluminescence (ECL kit, Pierce Biotechnology, Rockford, IL, USA). For estimation of small GTPase activation, lysis buffer including 50 mmol/L Tris (pH 7.5), 150 mmol/L NaCl, 10 mmol/L $MgCl_2$, 10 μg/mL aprotinin, 10 μg/mL leupeptin, 1 mmol/L phenylmethylsulfonyl fluoride, and 1% Triton X-100 was used. The amount of GTP-bound Rac1 and RhoA was analyzed by incubating total cell lysates with the p21-binding domain (PBD) of PAK-agarose beads or RhoA-binding domain (RBD) of Rhotekin-agarose beads. Following a 30 min incubation, the beads were washed and, after electrophoresis and blotting, membranes were probed with anti-Rac1 or anti-RhoA antibodies[13, 14].

Flow cytometry

Cells were detached with trypsin, centrifuged at 300×*g* for 4 min, washed with PBS, and counted. Cells (2×10^5) were centrifuged, and the pellet was then resuspended in PBS with 1% FBS and incubated with anti-active β1-integrin 12G10 antibodies for 30 min on ice. Cells were then extensively washed with PBS and incubated with the relevant (FITC-conjugated) secondary antibody for 20 min, washed, and analyzed using a flow cytometer (Becton Dickinson, Mountain View, CA, USA). Live cells were gated for the analysis and protein expression levels were analyzed using CELLQuest software.

Statistics

Data is presented as means±SEM. Statistical significance was analyzed by two-tailed Student's *t* test. The value of $P<0.05$ is considered significant.

Results

Heparanase stimulates CHO-K1 cell adhesion on fibronectin

Heparanase expression has been found to be related to cell adhesion potential. To investigate the effect of JG3 on heparanase-driven cell adhesion, CHO-K1 cells stably expressing heparanase were generated. Both Western blotting and RT-PCR analysis demonstrated a CHO-K1 cell line stably expressing heparanase (CHO-HPA) was successfully established (Figure 2A and 2B). We assayed one-hour adhesion on several extracellular matrixes. Heparanase overexpression stimulated CHO-K1 cell adhesion on fibronectin and vitronectin (Figure 2C), which, in turn, helps substantiate the fact that the CHO-HPA cell line functions as expected.

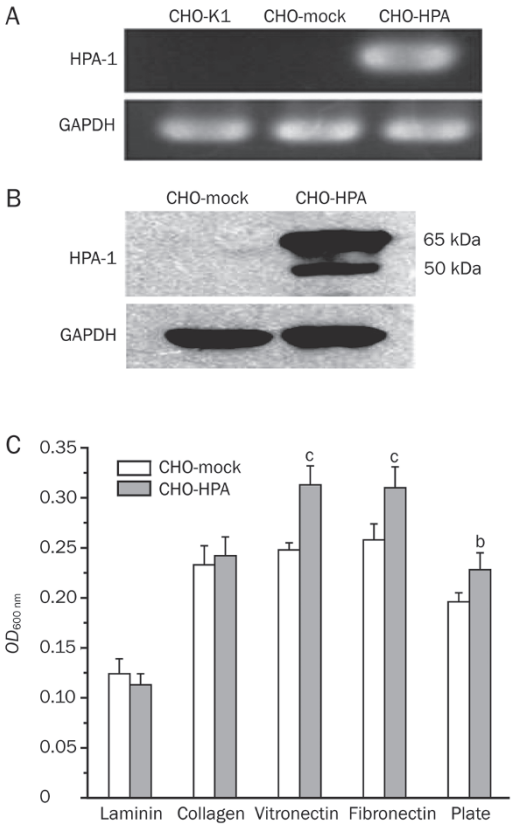

Figure 2. Heparanase stimulates CHO-K1 cells adhesion. (A) Western blotting results of the CHO-HPA cells with the control of empty vector transfected CHO-mock cells; (B) RT-PCR results of the CHO-HPA cells with the CHO-mock cells; (C) Heparanase-expressing cells showed better adhesion ability on fibronectin and vitronectin, but no significant differences were seen on laminin, collagen and non-extracellular matrix-coated plates. The graph represents the mean values±SD from three separate experiments. $^bP<0.05$; $^cP<0.01$ *vs* CHO-mock using an unpaired Student's *t* test.

JG3 abolishes the formation of focal adhesions in CHO-HPA cells

Because JG3 at 100 μg/mL was determined to be the most appropriate concentration in our previous *in vitro* studies, we used this concentration for subsequent experiments. To examine the effect of JG3 on the focal adhesion formation, we used an immunocytochemistry assay to detect the paxillin protein, a representative of the focal adhesion complex. Our results indicated that JG3 inhibited cell spreading and focal contact formation in CHO-HPA cells (Figure 3A). However, JG3 did not inhibit the attachment rates of CHO-HPA (Figure 3B).

JG3 fails to inhibit β1-integrin activation

The intimate involvement of integrins in cell adhesion and spreading has been well documented[15–19]. The $\alpha_4\beta_1$ integrin complex has been reported to be implicated in heparanase-mediated T-cell adhesion[20]. Moreover, this integrin complex functions as the main receptor of fibronectin[21, 22]. We therefore utilized a monoclonal antibody (12G10) that specifically recognizes the active state of β1-integrin to analyze β1-integrin

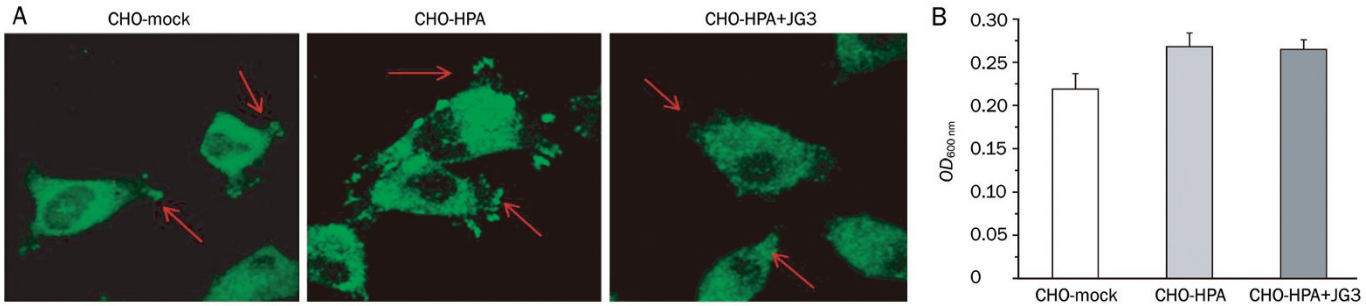

Figure 3. JG3 has inhibitory efficacy against heparanase-mediated cell adhesion. (A) The paxillin staining pattern shows that JG3 prevented the formation of focal adhesions in CHO-HPA cells. Photographs were taken under a confocal microscope (60×); (B) JG3 cannot inhibit the attachment rates of CHO-HPA cells. The graph indicates mean values±SD from three separate experiments.

activation by FACS. As indicated in Figure 4A, β1-integrin localization on the cell membrane was significantly higher in the CHO-HPA cells than in the CHO-mock cells. However, JG3 showed no marked impact on the activation of β1-integrin, nor any change in the expression level of β1-integrin (Figure 4B).

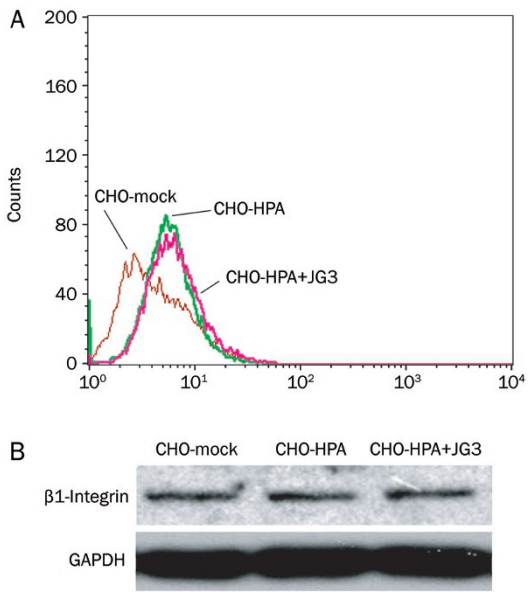

Figure 4. JG3 has no effect on β1-integrin activation and expression. (A) Heparanase expression induced β1-integrin activation, as detected by the 12G10 antibody, which specifically recognizes active β1-integrin, but treatment with JG3 did not affect the activation; (B) The β1-integrin protein was not influenced by JG3 treatment and heparanase expression.

JG3 suppresses cell adhesion signal transduction

Although β1-integrin activation was not affected by JG3, we cannot exclude the possibility that JG3 affects its downstream molecule(s) independently of the β1-integrin-targeting profile. To test this possibility, Src, FAK, and Erk1/2, the critical components in cell adhesion and spreading, were assessed. Western blot analysis revealed that a marked increase in phosphorylation of Src, FAK, and Erk1/2 was observed in CHO-HPA cells. Treatment with JG3 caused a significant down-regulation of FAK and Erk1/2 phosphorylation, while no change was observed in Src phosphorylation (Figure 5).

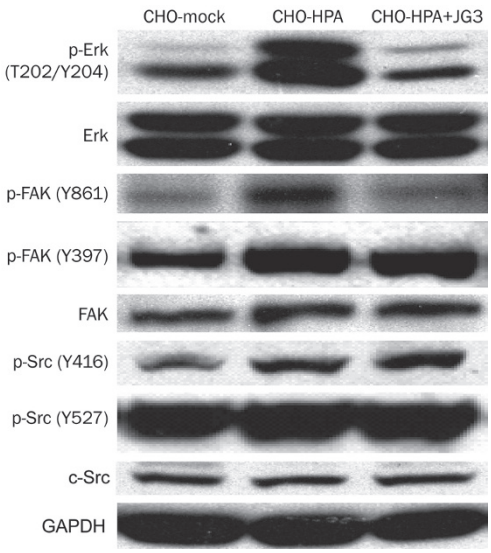

Figure 5. JG3 inhibits adhesion signal transduction. After being seeded on fibronectin for 1 h, CHO-HPA cells, as well as CHO-mock cells, were extracted and subjected to the Western blotting. Erk, FAK, and Src phosphorylation was stimulated by the overexpression of heparanase. Moreover, treatment with JG3 during the 1 h adhesion reduced Erk phosphorylation and FAK 861 site phosphorylation of CHO-HPA cells, while phosphorylation of Src was not affected.

JG3 inhibits cell motility mediated by heparanase

We next wondered whether JG3 had an inhibitory effect on filamentous actin. Using an immunocytochemistry assay, we found that JG3 significantly decreased the staining intensity of FITC-phalloidin labeled actin in CHO-HPA cells, as compared with the control (Figure 6A).

Small GTPases are thought to play instrumental roles in the early phases of cell adhesion and spreading. Cdc42 and Rac1 activation have been assumed to result in filopodia/lamellipodia extension and focal complex formation, while activation of

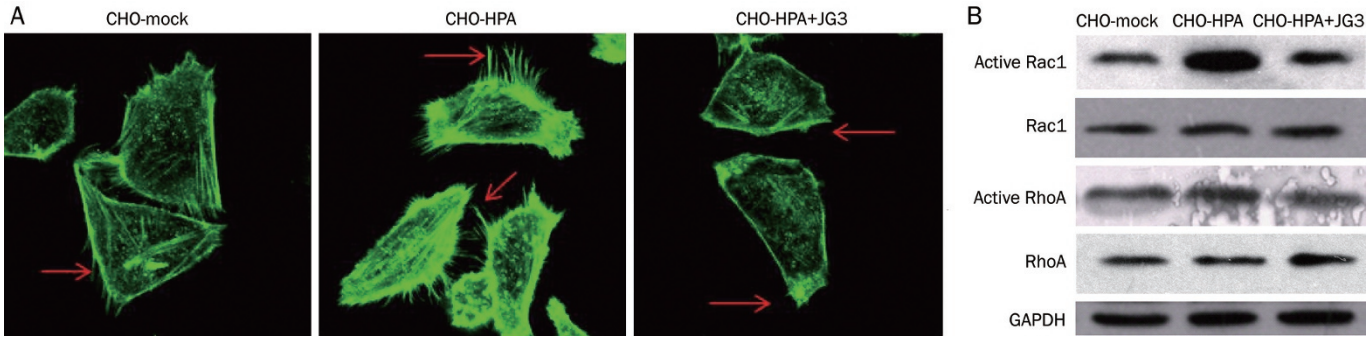

Figure 6. JG3 inhibits cell motility mediated by heparanase. (A) Heparanase stimulated cell adhesion and extension, and JG3 could neutralize this effect. Photographs were taken under a confocal microscope (×60); (B) Cells were washed with serum-free medium and were then seeded on fibronectin, with or without 100 μg/mL JG3. Cell lysates were then subjected to pull-down with GST-PAK-agarose beads and GST-Rhotekin-agarose beads for detection of active Rac1 (first panels) and active RhoA (third panels), as described in Materials and methods. Cell lysates were subjected to Western blotting with an anti-Rac1 antibody (second panels) and an anti-RhoA antibody (fourth panels). Heparanase expression increased Rac1 activation, and JG3 neutralized this effect. By contrast, any variation in RhoA activation was not obvious. The images are representative of three independent experiments.

RhoA induces the maturation of focal complexes to focal adhesions, assembly of stress fibers, and cell locomotion [23]. Therefore, we examined Rac1 and RhoA activation by employing agarose beads coupled to the RhoA-binding domain (RBD) of Rhotekin, and the p21 binding domain (PBD) of p21-activated protein kinase (PAK), domains which specifically bind the active, GTP-bound form of RhoA and Rac1, respectively[13, 14]. We found that Rac1 activation was markedly induced in the heparanase-expressed cells, and this activation was significantly reversed by the treatment of JG3. The effect of JG3 on RhoA activation was not obvious (Figure 6B), and no change was observed in Cdc42 (data not shown).

Discussion

Adhesion and subsequent spreading are crucial steps involved in metastasis. Metastatic spreading is a severe complication of neoplastic disease that is responsible for most cancer-related deaths. Besides its role in metastasis and angiogenesis, heparanase was further noted to enhance cell adhesion via activation of β1-integrin and Rac1[9, 10]. A recent paper[24] underscored the idea that the pro-adhesive properties of heparanase were mediated by its interaction with cell surface heparan sulfate proteoglycans (HSPG) via the KKDC domain on heparanase. This subsequently results in clustering of syndecan-1 and syndecan-4, which initiates signaling cascades involving Rac1 and the PKC pathways.

In the present study, we found that heparanase-overexpressing CHO-K1 cells showed better spreading profiles and formed more focal contacts; furthermore, these properties were accompanied by the activation of FAK and Erk and Rac1. Encouragingly and expectedly, these features can be significantly inhibited by the treatment with JG3. The fact that JG3 is capable of binding to the KKDC domain of heparanase[12], together with its marked inhibition of syndecan clustering (unpublished data), help us understand the mechanisms underlying the inhibitory action of JG3 on cell motility, and thus how it may contribute to the inhibition of metastasis.

Taken together, our results provide further evidence to support a notion that JG3 functions as a promising new compound for cancer therapy.

Acknowledgements

This work was supported by Natural Science Foundation of China for Distinguished Young Scholars (30725046) and the Natural Science Foundation of China for Innovation Research Group (30721005).

Author contribution

Qiu-ning LI, Hai-ying LIU and Mei-yu GENG designed the experiments. Qiu-ning LI, Qiu-ming PAN and Lu WANG performed the experiments. Qiu-ning LI and Xian-liang XIN analyzed data and wrote the manuscript. Qin CHEN and Jing ZHANG contributed many reagents and suggestions. Mei-yu GENG and Jian DING revised the manuscript.

References

1 Nakajima M, Irimura T, Di Ferrante N, Nicolson GL. Metastatic melanoma cell heparanase. Characterization of heparan sulfate degradation fragments produced by B16 melanoma endoglucuronidase. J Biol Chem 1984; 259: 2283–90.
2 Bar-Ner M, Kramer MD, Schirrmacher V, Ishai-Michaeli R, Fuks Z, Vlodavsky I. Sequential degradation of heparan sulfate in the subendothelial extracellular matrix by highly metastatic lymphoma cells. Int J Cancer 1985; 35: 483–91.
3 Nakajima M, Irimura T, Di Ferrante D, Di Ferrante N, Nicolson GL. Heparan sulfate degradation: relation to tumor invasive and metastatic properties of mouse B16 melanoma sublines. Science 1983; 220: 611–3.
4 Vlodavsky I, Fuks Z, Bar-Ner M, Ariav Y, Schirrmacher V. Lymphoma cell-mediated degradation of sulfated proteoglycans in the subendothelial extracellular matrix: relationship to tumor cell metastasis. Cancer Res 1983; 43: 2704–11.
5 McKenzie EA. Heparanase: a target for drug discovery in cancer and

inflammation. Br J Pharmacol 2007; 151: 1–14.
6 Sanderson RD, Yang Y, Suva LJ, Kelly T. Heparan sulfate proteoglycans and heparanase-partners in osteolytic tumor growth and metastasis. Matrix Biol 2004; 23: 341–52.
7 Miao HQ, Liu H, Navarro E, Kussie P, Zhu Z. Development of heparanase inhibitors for anti-cancer therapy. Curr Med Chem 2006; 13: 2101–11.
8 Vlodavsky I, Abboud-Jarrous G, Elkin M, Naggi A, Casu B, Sasisekharan R, *et al.* The impact of heparanese and heparin on cancer metastasis and angiogenesis. Pathophysiol Haemost Thromb 2006; 35: 116–27.
9 Zetser A, Bashenko Y, Miao HQ, Vlodavsky I, Ilan N. Heparanase affects adhesive and tumorigenic potential of human glioma cells. Cancer Res 2003; 63: 7733–41.
10 Goldshmidt O, Zcharia E, Cohen M, Aingorn H, Cohen I, Nadav L, *et al.* Heparanase mediates cell adhesion independent of its enzymatic activity. FASEB J 2003; 17: 1015–25.
11 Sotnikov I, Hershkoviz R, Grabovsky V, Ilan N, Cahalon L, Vlodavsky I, *et al*. Enzymatically quiescent heparanase augments T cell interactions with VCAM-1 and extracellular matrix components under versatile dynamic contexts. J Immunol 2004; 172: 5185–93.
12 Zhao H, Liu H, Chen Y, Xin X, Li J, Hou Y, *et al.* Oligomannurarate sulfate, a novel heparanase inhibitor simultaneously targeting basic fibroblast growth factor, combats tumor angiogenesis and metastasis. Cancer Res 2006; 66: 8779–87.
13 Ren XD, Kiosses WB, Schwartz MA. Regulation of the small GTP-binding protein Rho by cell adhesion and the cytoskeleton. EMBO J 1999; 18: 578–85.
14 Ren XD, Schwartz MA. Determination of GTP loading on Rho. Methods Enzymol 2000; 325: 264.
15 Varner JA, Cheresh DA. Integrins and cancer. Curr Opin Cell Biol 1996; 8: 724–30.
16 Giancotti FG. Integrin signaling: specificity and control of cell survival and cell cycle progression. Curr Opin Cell Biol 1997; 9: 691–700.
17 Brakebusch C, Bouvard D, Stanchi F, Sakai T, Fassler R. Integrins in invasive growth. J Clin investigation 2002; 109: 999–1006.
18 Damsky CH, Ili D. Integrin signaling: it's where the action is. Curr Opin Cell Biol 2002; 14: 594–602.
19 Howe AK, Aplin AE, Juliano RL. Anchorage-dependent ERK signaling-mechanisms and consequences. Curr Opin Genet Dev 2002; 12: 30–5.
20 Gilat D, Hershkoviz R, Goldkorn I, Cahalon L, Korner G, Vlodavsky I, *et al.* Molecular behavior adapts to context: heparanase functions as an extracellular matrix-degrading enzyme or as a T cell adhesion molecule, depending on the local pH. J Exp Med 1995; 181: 1929–34.
21 Sánchez-Aparicio P, Dominguez-Jiménez C, Garcia-Pardo A. Activation of the alpha 4 beta 1 integrin through the beta 1 subunit induces recognition of the RGDS sequence in fibronectin. J Cell Biol 1994; 126: 271–9.
22 Sechler JL, Cumiskey AM, Gazzola DM, Schwarzbauer JE. A novel RGD-independent fibronectin assembly pathway initiated by alpha4beta1 integrin binding to the alternatively spliced V region. J Cell Sci 2000; 113 (Pt 8): 1491–8.
23 Burridge K, Wennerberg K. RhoA and Rac take center stage. Cell 2004; 116: 167–79.
24 Levy-Adam F, Feld S, Suss-Toby E, Vlodavsky I, Ilan N. Heparanase facilitates cell adhesion and spreading by clustering of cell surface heparan sulfate proteoglycans. PLoS ONE 2008; 3: e2319.